Available online at www.sciencedirect.com
ScienceDirect
Journal of Power Sources 165 (2007) 97–101
JOURNAL OF POWER SOURCES
www.elsevier.com/locate/jpowsour

Short communication

Electrochemical performance of $(Ba_{0.5}Sr_{0.5})_{0.9}Sm_{0.1}Co_{0.8}Fe_{0.2}O_{3-\delta}$ as an intermediate temperature solid oxide fuel cell cathode

Shuyan Li [a,*], Zhe Lü [a], Na Ai [a], Kongfa Chen [a], Wenhui Su [a,b,c,**]

[a] *Center for the Condensed-Matter Science and Technology, Harbin Institute of Technology, Harbin 150001, PR China*
[b] *Department of Condensed Matter Physics, Jilin University, Changchun 130023, PR China*
[c] *International Centre for Materials Physics, Academia Sinica, Shenyang 110015, PR China*

Received 15 July 2006; received in revised form 8 November 2006; accepted 17 November 2006
Available online 10 January 2007

Abstract

This study presents the electrochemical performance of $(Ba_{0.5}Sr_{0.5})_{0.9}Sm_{0.1}Co_{0.8}Fe_{0.2}O_{3-\delta}$ (BSSCF) as a cathode material for intermediate temperature solid oxide fuel cells (IT-SOFC). AC-impedance analyses were carried on an electrolyte supported BSSCF/$Sm_{0.2}Ce_{0.8}O_{1.9}$ (SDC)/Ag half-cell and a $Ba_{0.5}Sr_{0.5}Co_{0.8}Fe_{0.2}O_{3-\delta}$ (BSCF)/SDC/Ag half-cell. In contrast to the BSCF cathode half-cell, the total resistance of the BSSCF cathode half-cell was lower, e.g., at 550 °C; the values for the BSSCF and BSCF were 1.54 and 2.33 Ω cm^2, respectively. The cell performance measurements were conducted on a Ni-SDC anode supported single cell using a SDC thin film as electrolyte, and BSSCF layer as cathode. The maximum power densities were 681 mW cm^{-2} at 600 °C and 820 mW cm^{-2} at 650 °C.

Keywords: Intermediate-temperature solid oxide fuel cell; $Sm_{0.2}Ce_{0.8}O_{1.9}$; Cathode material; AC-impedance; Perovskite oxide

1. Introduction

With the increasing attention to the IT-SOFC, finding one kind of cathode material with good performance at the lower temperature is believed to be the key to enhancing the power density [1,2]. Co-based perovskite compounds are the main cathodes for the IT-SOFC because of their mixed-conductor characteristics and higher ion-conductivity [3,4]. Especially, the composition of BSCF presented as a cathode material, improves the performance of both dual-chamber and single-chamber configurations at low temperatures further. This material provides a high rate of oxygen ion diffusion following oxygen reduction. But its electrical conductivity is lower, for example, at 600 °C. The electrical conductivity values for $La_{1-x}Sr_xCo_{0.2}Fe_{0.8}O_3$ (LSCF) and BSCF are 330 and 28 S cm^{-1}, respectively [5–8], which is not beneficial to cathode performance. So in our earlier work, Sm was introduced in the A-site of BSCF composing "BSSCF" to enhance the electrical conductivity and we succeeded. The improved electrical conductivity can get to 215 S cm^{-1} at 400 °C, and is attributed to the increased concentration of electronic charge carriers because of the reduction of Co^{4+}, Fe^{4+} [9].

In the present study, the AC-impedance spectra of the BSSCF cathode was investigated on the cathode/electrolyte half-cell (BSSCF/SDC/Ag) and was compared with a BSCF cathode half-cell (BSCF/SDC/Ag). Then, the performance of the anode supported single cell using BSSCF as the cathode material, SDC thin film as electrolyte (BSSCF/SDC/NiO-SDC) was evaluated.

2. Experiment

2.1. preparations of powder

$(Ba_{0.5}Sr_{0.5})_{0.9}Sm_{0.1}Co_{0.8}Fe_{0.2}O_{3-\delta}$ (BSSCF) powder was prepared by the EDTA-citric acid complexing method. Powders of $Ba(NO_3)_2$ (>99.5%), $Sr(NO_3)_2$ (>99.5%), $Co(NO_3)_2{\cdot}6H_2O$ (>97.0%), $Fe(NO_3)_3{\cdot}9H_2O$ (>98.5%), Sm_2O_3 and EDTA (ethylenediamine tetraacetic acid, >99.5%), citric acid (>99.5%) were weighed in stoichiometric proportions and mixed together in a water bath at a temperature of 80 °C. Then they were

* Corresponding author. Tel.: +86 451 86401150.
** Corresponding author at: Center for the Condensed-Matter Science and Technology, Harbin Institute of Technology, Harbin 150001, PR China. Tel.: +86 451 86418440; fax: +86 451 86412828.
E-mail addresses: lsy614@21cn.com (S. Li), suwenhui@hit.edu.cn (W. Su).

0378-7753/$ – see front matter © 2006 Elsevier B.V. All rights reserved.
doi:10.1016/j.jpowsour.2006.11.022

dissolved completely, a certain amount of citric acid was introduced, and the mole ratio of EDTA acid: Citric acid: total metal ions was controlled around 1:1.5:1. Mild heating induced gelation of the solution, and the resulting gel was held at 200 °C for several hours to remove organics. Lastly, the primary powders were calcined at 950 °C for 5 h [9–13]. The $Sm_{0.2}Ce_{0.8}O_{1.9}$ (SDC) powders were prepared using a glycine-nitrate process and calcined at 800 °C for 2 h in this study [14]. Nickel oxide (NiO) powders were synthesized by the precipitation method, using Ni $(NO_3)_2{\cdot}6H_2O$ as the material and ammonia as the precipitant. The resultant powder was calcined at 400 °C for 2 h.

2.2. Electrochemical testing

Electrochemical testing in this study was carried out using AC-impedance and the three-electrode method. The SDC powder was compacted under uniaxial pressure (200 Mpa) to form a disc (0.4 mm in thickness). After pre-sintering at 1000 °C, the surface of the SDC disc was coarsened by spraying a SDC layer as a roughness treatment, and then sintered at 1400 °C for 4 h. The BSSCF powder mixture was dispersed in terpineol and spread on the coarsened electrolyte surface used as the working electrode (WE) and reference electrode (RE), then sintered at 1050 °C for 4 h in air. A silver counter electrode (CE) was arranged on the other side of the electrolyte disk using DAD87 silver paste then pyrolysis.

The measurements of AC-impedance spectra were performed at 400, 450, 500 and 550 °C using an Impedance/Gain-phase Analyzer (Solartron SI 1260) with a 10 mV ac signal, over a 0.1 Hz–910 kHz frequency range.

The microstructure of the BSSCF/SDC half-cell was studied by SEM.

2.3. Single cell fabrication and testing

The anode powders were prepared by mixing together NiO, SDC powders and flour in a weight ratio of 65:35:20, followed by ball-milling. After drying, the anode powders were subsequently pressed then calcined at 1000 °C for 2 h as substrates. A multilayer SDC film was prepared on the anode substrate using a slurry spin coating technique, and then a bilayer of SDC film/NiO-SDC anode was co-sintered at 1400 °C for 4 h. A slurry containing the BSSCF powders, ethyl cellulose and terpineol, was spin coated on the SDC film to form the cathode layer, followed by sintering at 1050 °C for 4 h. The substrate-electrolyte bilayer was sealed at one end of an alumina tube by applying a silver paste (DAD-87) to form a single cell, as shown in Fig. 1. This cell was heated in a furnace gradually to 650 °C to reduce the NiO on the anode support to Ni, and then the performance was tested by the four-probe method from 500 to 650 °C. Dry hydrogen was used as the fuel and the cathode was exposed to stationary air. The cell output performance and electrochemical impedance spectra were measured with a SI 1278 electrochemical interface (Solartron Instruments, Hampshire, UK) and SI 1260 Impedance/Gain-phase Analyzer, respectively.

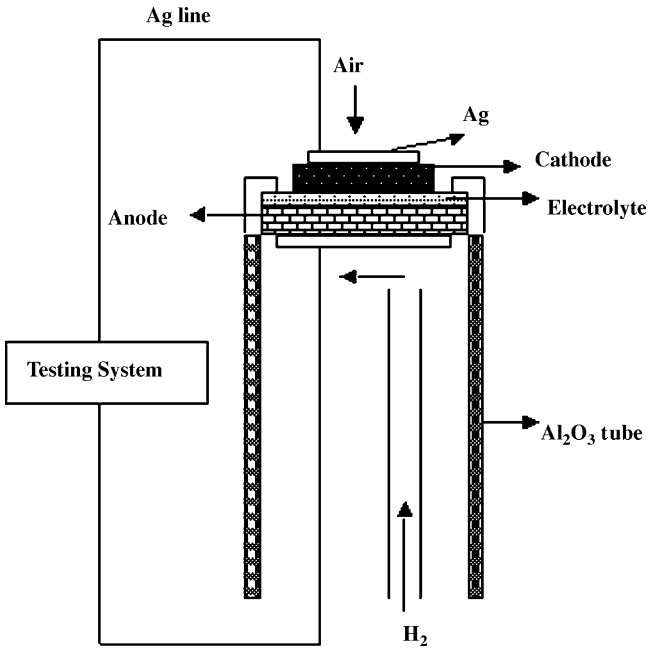

Fig. 1. Illustration of the single cell.

3. Result and discussion

3.1. Microstructure characterization

The micrographs of the cross-section views of electrolyte-supported BSSCF/SDC half-cell as well as the surface of cathode are shown in Fig. 2(a) and (b), respectively. It can be seen that the electrolyte is dense, and the cathode is fabricated in a high porosity structure to assure gas diffusion. Due to the surface roughness treatment of SDC, the connection between SDC and BSSCF cathode was good, as shown in Fig. 2(a).

3.2. Impedance spectra

Fig. 3(a) and (b) show the impedance spectra of the electrolyte supported half-cell using BSCF and BSSCF as cathode, respectively, from 400 to 550 °C in air. The equivalent circuit is presented in Fig. 3(c), and the fitting results of the resistance for the two materials using the Zview program (Scribner Associates, Inc.) are shown in Fig. 4.

As shown in Fig. 3, the impedance spectra consisted of two depressed semi-circles. This indicates that there are at least two electrode processes corresponding to the two semi-circles during molecular oxygen reduction. According to Heuveln and Bouwmeester [15] and Leng et al's works [16], the high frequency semi-circle can be attributed to the polarization during charge transfer. On the other hand, the low frequency semi-circle can be attributed to oxygen adsorption and desorption on the electrode surface and the diffusion of the oxygen ions. Therefore, in the equivalent circuit, the R_1 is denoted as the ohmic resistance including the electrolyte resistance between the working electrode and reference electrode, as well as the DC resistance of leads and electrode. The resistance R_2 is interpreted as the

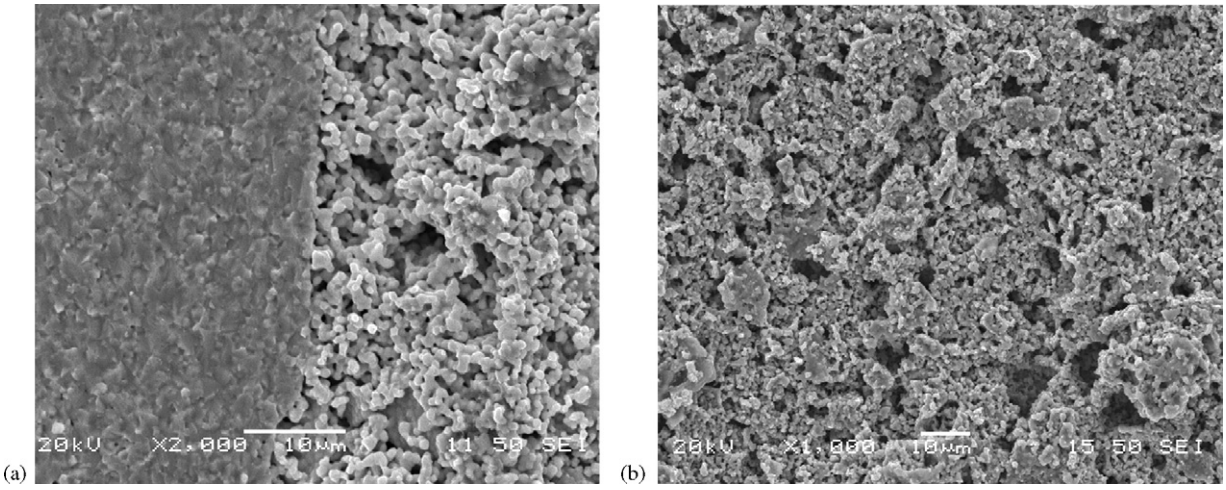

Fig. 2. (a) SEM cross-section image of the half-cell (BSSCF as cathode and SDC as electrolyte) (b) SEM top view of the cathode (BSSCF) layer.

charge transfer resistance, which is contributed by the electrochemical reaction at cathode–electrolyte interface. The Warburg impedance (W_1) in the equivalent circuit is related to the resistance of oxygen adsorption/decomposition and the oxygen ions diffusion in the cathode [17]. It can be seen in Fig. 4 that the total resistance (R_{el}) of BSSCF is lower than that of BSCF. Thus the doped of Sm in A-site not only enhances the electrical conductivity, but also lowers the cathode resistance [9]. Furthermore, the resistance of oxygen diffusion (W_1) governs the total resistance (R_{el}), and the decrease of total resistance is mainly the result of its reduction.

For mixed conductors like BSCF and BSSCF, the oxygen reduction occurs on not only the TPBs but also the surface and inside of the electrode [9]. On the electrode surface, the adsorbed molecular oxygen is decomposed, and then takes up oxygen vacancies, obtaining electrons to become lattice oxygen. Through transportation, the lattice oxygen goes into the crystal lattice, and at the same time, oxygen vacancies diffuse from the interface of electrode/electrolyte to the surface reaction region. In this process, the resistance of the oxygen adsorption/decomposition and mass transfer is the main part of the total resistance, so reducing the resistance of oxygen diffusion effectively is important for the reduction of total resistance [17,18]. For the BSSCF material, the doped of Sm^{3+} enhances the average valence of A-sites, inducing the reduction of Co^{4+} and Fe^{4+} to maintain the charge balance. This benefits the diffusion of oxygen in BSSCF and lowers the resistance to oxygen diffusion, and therefore reduces the total resistance obviously.

Fig. 5 shows the Arrhenous plots of the diffusion resistance (W_1) for BSCF and BSSCF cathodes, the activation energies of oxygen diffusion obtained from the slope of the fitted line are 88.79 and 70.51 kJ mol^{-1}, respectively. The value of BSSCF is lower than that of BSCF, which means the doping with Sm indeed reduces the activation energy for oxygen diffusion, and so accelerates oxygen diffusion. In addition, the activation energies of total cathode resistance (R_{el}) were also calculated, BSSCF: $E_a = 75.62$ kJ mol^{-1}, BSCF: $E_a = 89.55$ kJ mol^{-1}, are shown in Fig. 6.

3.3. Performance evaluation

Fig. 7 shows the variation of cell voltage and power density as a function of current density for the BSSCF/SDC/NiO-SDC cell under 30 mL min^{-1} of hydrogen from 500 to 650 °C. As seen in Fig. 7, the power density increases with increasing the operating temperature. Maximum power densities of the cell are 268, 442, 681 and 820 mW cm^{-2} at 500, 550, 600 and 650 °C, respectively. The excellent performance of the cell illustrates that the BSSCF is a good choice for IT-SOFC cathode material.

Fig. 8 shows the AC-impedances of the cell under open-circuit conditions (OCV). The total resistance contains the interfacial resistance and the ohmic resistance, which are determined from the impedance spectra and shown in Table 1. All kinds of resistances decrease with increasing temperature, and the total resistance of the cell is mainly governed by the interfacial resistance, from 62.3% at 650 °C to 86.6% at 500 °C. Furthermore, the interfacial resistance of the anode–electrolyte is relative small [19,20], thus the interfacial resistance is mainly from the cathode–electrolyte interface. So reducing the cathode–electrolyte interface resistance is the key to reducing the total resistance as well as to improve the performance of the cell [14].

In addition, it is observed that the resistances of the single cell (BSSCF/SDC/NiO-SDC) are lower than that of the half-cell BSSCF/SDC/Ag. For example, at 550 °C the total resistances of the single cell and half-cell are 0.45 and 1.54 Ω cm^2, respectively. It is considered that the difference is mainly caused by two reasons: (1) the electronic conductivity of electrolyte film (SDC) (2) the atmosphere in which the SDC works in.

Table 1
Fitted impedance spectra values for single cell BSSCF/SDC/NiO-SDC (Ω cm^2)

	Temperature			
	500 °C	550 °C	600 °C	650 °C
Interface resistance	1.010	0.360	0.140	0.074
Ohmic resistance	0.160	0.090	0.074	0.045
Total resistance	1.170	0.450	0.210	0.120

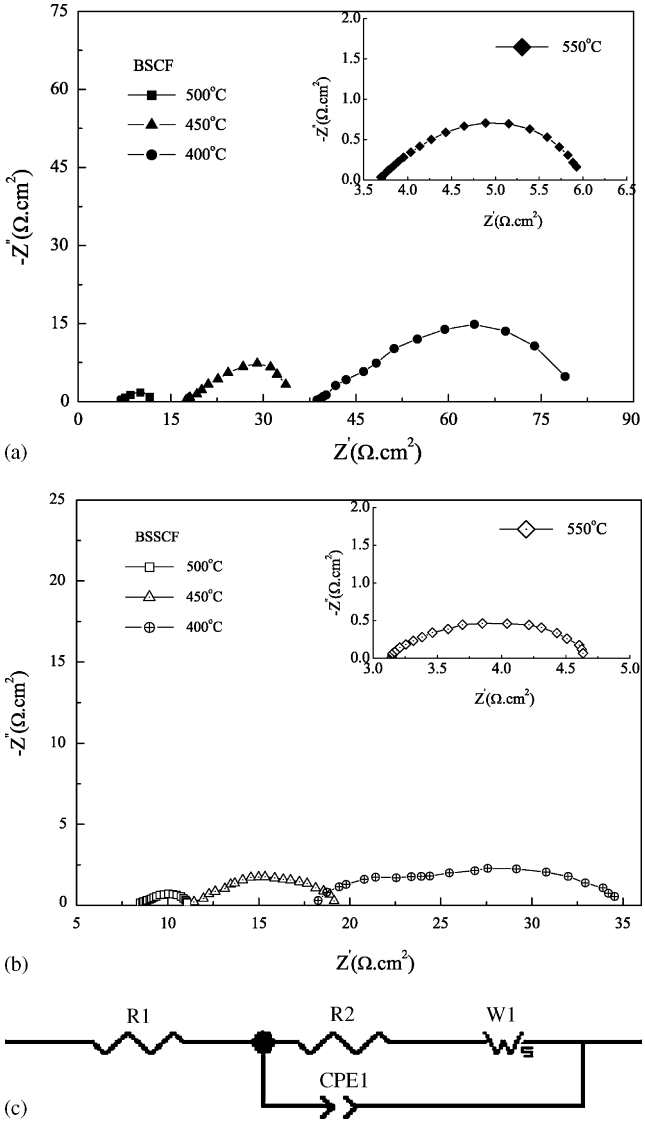

Fig. 3. (a) Impedance spectra of BSCF at 400,450,500 and 550 °C. (b) Impedance spectra of BSSCF at 400,450,500 and 550 °C (c) Equivalent circuit model. R_1: ohmic resistance; R_2: charge transfer resistance; W_1: oxygen adsorption/decomposition resistance and oxygen diffusion resistance; CPE_1: constant phase element.

Firstly, because of the mixed conductivity characteristic of SDC, the electronic conduction in the SDC film is not negligible. Thus, even under the condition of OCV, the cell can discharge through the electronic resistance. Therefore, there is still an electric current in the cell under this condition [17,18]. Actually, the cell was under a polarization condition when the AC-impedances were measured. It is expected that the reduction of the molecular oxygen to oxygen ions as well as the oxygen ion concentration around the reaction region can be greatly enhanced by the electric current [17,21,22]. Therefore, a decrease of oxygen diffusion resistance can be expected.

Secondly, the different atmosphere where the half-cell and the single cell work is another reason causing the difference of resistance. For the half-cell, the whole electrolyte (SDC) as well as the electrode is in the stationary air. While for the cell, the mixed atmosphere (H_2/air) where the cell works in has an

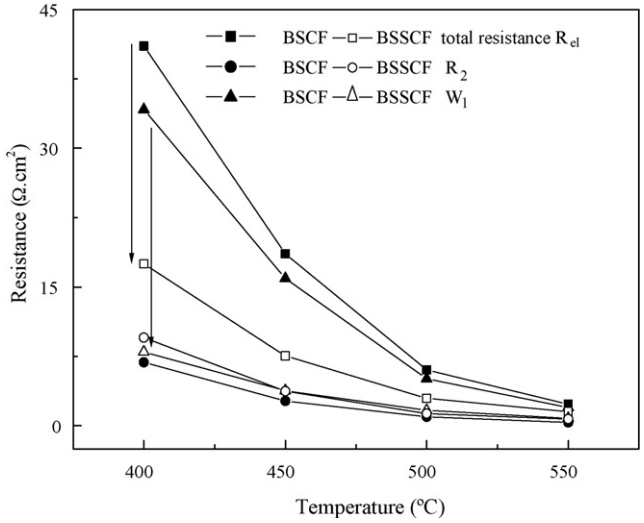

Fig. 4. The total resistance (R_{el}), charge transfer resistance (R_2) and oxygen diffusion resistance (W_1) of BSCF and BSSCF.

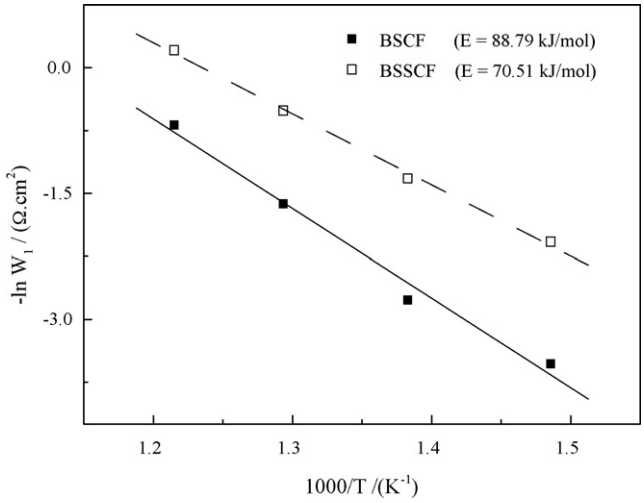

Fig. 5. Arrhenius plots of the diffusion conductance (W_1) for BSCF and BSSCF cathode from 400 to 550 °C.

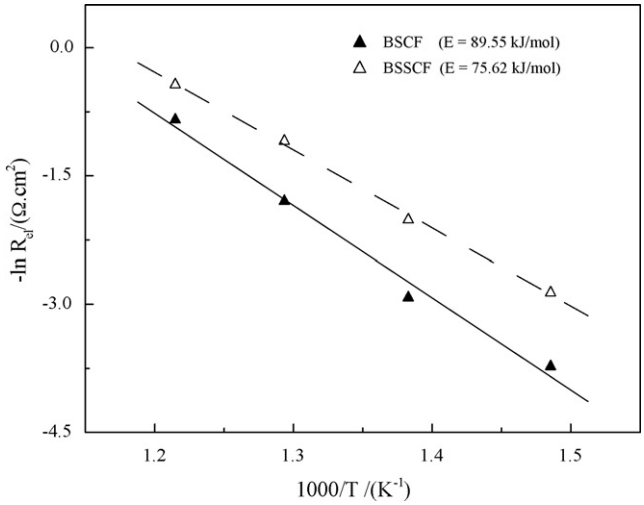

Fig. 6. Arrhenius plots of the total conductance (R_{el}) for BSCF and BSSCF cathode from 400 to 550 °C.

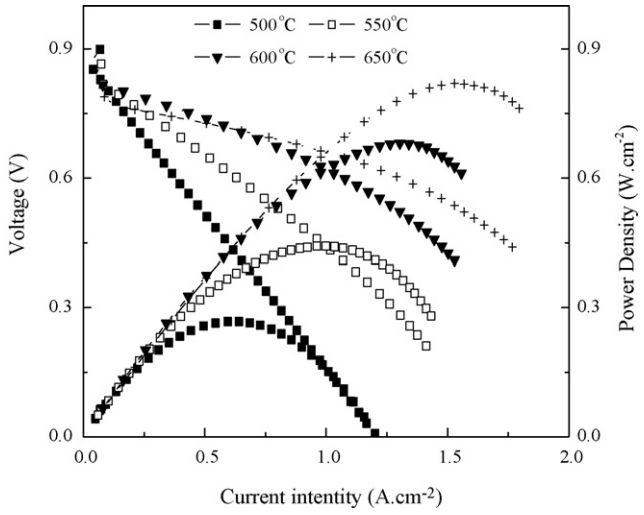

Fig. 7. Performance of the cell (BSSCF/SDC/NiO-SDC) from 500 to 650 °C.

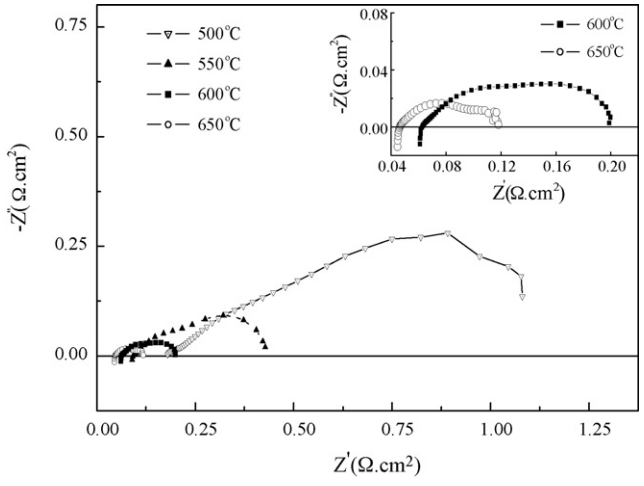

Fig. 8. The impedance spectra of the cell (BSSCF/SDC/NiO-SDC) measured under open-circuit condition.

effect on the performance of the SDC film, which influences the resistance. The effect of atmosphere on the cell performance will been investigated in detail in the future.

Since the cathode–electrolyte interface resistance is the main reason affecting the single cell performance, a modified BSSCF by addition of high ionic conductivity electrolyte material to increase oxygen ion pathways should yield better performance. The high thermal expansion coefficient of BSSCF will induce the cathode to delaminate during the sintering and measuring processes, so an additional porous interlayer of electrolyte can be deposited between the cathode and the film layer as coarse layer to enhance the performance.

4. Conclusion

In this study, the electrochemical characterization and performance of IT-SOFC using $(Ba_{0.5}Sr_{0.5})_{0.9}Sm_{0.1}Co_{0.8}Fe_{0.2}O_{3-\delta}$ as a cathode material was investigated. The impedance spectra were measured on the BSSCF/SDC/Ag half-cell as well as on the BSCF/SDC/Ag half-cell. The resistance values of the BSSCF cathode were lower than the BSCF cathode, e.g. at 550 °C, the values for BSSCF and BSCF were 1.54 and 2.33 $\Omega\,cm^2$, respectively. This indicates that the doping of Sm in the BSSCF lowers the resistance to oxygen diffusion effectively and thus reduces the total resistance. For the performance testing carried out on a BSSCF/SDC/NiO-SDC single cell, the maximum power densities obtained were 268, 442, 681 and 820 mW cm^{-2} at 500, 550, 600 and 650 °C. The total resistances of the cell were 1.17, 0.45, 0.21 and 0.12 $\Omega\,cm^2$ respectively. These results illustrate that BSSCF is a good choice for the IT-SOFC cathode material. In future investigations, the BSSCF compositional modification and microstructure optimization of the interface of cathode/electrolyte film will be adopted.

References

[1] X.Y. Xu, C.R. Xia, G.L. Xiao, D.K. Peng, Solid State Ionics 176 (2005) 1513–1520.
[2] E. Maguire, B. Gharbage, F.M.B. Marques, J.A. Labrincha, Solid State Ionics 127 (2000) 329–335.
[3] A. Petric, P. Huang, F. Tietz, Solid State Ionics 135 (2000) 719–725.
[4] A. Hartley, M. Sahibzada, M. Meston, I.S. Metcalfe, D. Mantzavinos, Catal. Today 55 (2000) 197–204.
[5] Z.P. Shao, S.M. Halle, Nature 431 (2004) 170–173.
[6] B. Wei, Z. Lü, S.Y. Li, Y.Q. Liu, K.Y. Liu, W.H. Su, Electrochem. Solid State Lett. 8 (2005) A428–A431.
[7] L.W. Tai, M.M. Nasrallah, H.U. Anderson, D.M. Sparlin, S.R. Sehlin, Solid State Ionics 76 (1995) 259–271.
[8] L.W. Tai, M.M. Nasrallah, H.U. Anderson, D.M. Sparlin, S.R. Sehlin, Solid State Ionics 76 (1995) 273–283.
[9] S.Y. Li, Z. Lü, B. Wei, X.Q. Huang, J.P. Miao, G. Cao, W.H. Su, J. Alloys Compd. 426 (2006) 408–414.
[10] H.H. Wang, R. Wang, D.T. Liang, W.S. Yang, J. Membr. Sci. 243 (2004) 405–415.
[11] L. Tan, X.H. Gu, L. Yang, W.Q. Jin, L.X. Zhang, N.P. Xu, J. Membr. Sci. 212 (2003) 157–165.
[12] L. Tan, X.H. Gu, L. Yang, L.X. Zhang, C.Q. Wang, N.P. Xu, Sep. Purif. Technol. 32 (2003) 307–312.
[13] Z.P. Shao, W.S. Yang, Y. Cong, H. Dong, J.H. Tong, G.X. Xiong, J. Membr. Sci. 172 (2000) 177–188.
[14] N. Ai, Z. Lü, K.F. Chen, X.Q. Huang, B. wei, Y.H. Zhang, S.Y. Li, X.H. Xin, X.Q. Sha, W.H. Su, J. Power Sources 159 (2006) 637–640.
[15] F.H. Heuveln, H.J.M. Bouwmeester, J. Electrochem. Soc. 144 (1997) 134–137.
[16] Y.J. Leng, S.H. Chan, K.A. Khor, S.P. Jiang, Int. J. Hydrogen Energy 29 (2004) 1025–1033.
[17] H.-C. Yu, F. Zhao, A.V. Virkar, K.-Z. Fung, J. Power Sources 152 (2005) 22–26.
[18] C.R. Xia, W.L. Rauch, F.L. Chen, M.L. Liu, Solid State Ionics 149 (2002) 11–19.
[19] S. de Souza, S.J. Visco, L.C. De Jonghe, J. Electrochem. Soc. 144 (1997) L35–L37.
[20] C.R. Xia, M.L. Liu, Solid State Ionics 152/153 (2002) 423–430.
[21] J. Van herle, R. Ihringer, R. Vasquez Cavieres, L. Constantin, O. Bucheli, J. Eur. Ceram. Soc. 21 (2001) 1855–1859.
[22] S.P. Jiang, J.G. Love, J.P. Zhang, M. Hoang, Y. Ramprakash, A.E. Hughes, S.P.S. Badwal, Solid State Ionics 121 (1999) 1–10.